Available online at www.sciencedirect.com
ScienceDirect
Chemical Physics Letters 452 (2008) 99–104
CHEMICAL PHYSICS LETTERS
www.elsevier.com/locate/cplett

Picosecond to nanosecond reorganization of water in AOT/lecithin mixed reverse micelles of different morphology

S. Shankara Narayanan, Sudarson Sekhar Sinha, Rupa Sarkar, Samir Kumar Pal *

Unit for Nano Science and Technology, Department of Chemical, Biological and Macromolecular Sciences, S. N. Bose National Centre for Basic Sciences, Block JD, Sector III, Salt Lake, Kolkata 700 098, India

Received 24 October 2007; in final form 13 December 2007
Available online 23 December 2007

Abstract

We report the effect of different geometrical restrictions on the dynamical properties of water using dynamic light scattering (DLS), Fourier transform infrared (FTIR) and picosecond-resolved fluorescence studies. By preparing AOT/lecithin mixed reverse micelles (RMs) of different morphologies (spherical and ellipsoidal), we have investigated the effect of the degree of confinement on the mobility of water in the mixed RMs of similar degree of hydration. The FTIR studies along with solvation dynamics of two fluorescent probes, ANS and coumarin 500 in the RMs reveal structural and dynamical information about the micellar water, which varies with the morphology of the mixed RMs.

1. Introduction

The dynamical aspects of confined water in nanosize organized molecular assemblies, including micelles and reverse micelles (RMs), have drawn considerable attention in the recent past [1–5], showing that a number of water properties differ significantly in nanoscopic confinement from those in the bulk water. Dynamical studies of water in RM [1,6] using pump–probe IR spectroscopy exhibit different orientational relaxation time of highly immobile interface-solvating water and fast moving bulk-like core water in the picosecond (1–100 ps) time scale. Several research groups [1,7–9] have investigated the dynamical response of water in the nanopool of AOT RMs. Molecular dynamics (MD) simulations have also revealed different structural and dynamical properties of water in RMs [10–12]. Polar solvation dynamics in ionic and nonionic RMs has been reported through a series of publications from Levinger's group [2,3,7,13] using a fluorescent probe coumarin 343. A slow relaxation of water molecules has been demonstrated inside the nanopool of RMs regardless of the characteristics of counterion. They have also studied the influence of morphology on the solvation dynamics of water in lecithin reverse micelle [14]. However, a detailed structural study on the RMs with different morphology is lacking in the literature. Limited experimental time window (500 ps) in the study also restricts to explore the nanosecond solvation dynamics, which essentially reflects the translational motion of water in the organized assembly.

In the present study, we have investigated the picosecond to nanosecond dynamics of water in RMs of different morphologies (spherical and ellipsoidal). A mixture of two surfactants has been used to prepare RMs of different shapes with similar degrees of hydration. The presence of co-surfactants in mixed surfactant system in a nonpolar solvent permits different microstructures and morphologies [15,16], which are not possible in the case of single surfactant systems. Dynamic light scattering (DLS) studies have been performed to track the alteration of the shape of the RMs with varying [AOT]:[lecithin]. Another important issue in the RMs with mixed surfactants is the structure of water molecules in the confined nanopools. Although efforts have been made to a large extent to investigate the structure of water molecules in single surfactant assembly using different techniques [1,13,17,18], the structure of

* Corresponding author. Fax: +91 33 2335 3477.
E-mail address: skpal@bose.res.in (S.K. Pal).

0009-2614/$ - see front matter © 2007 Elsevier B.V. All rights reserved.
doi:10.1016/j.cplett.2007.12.040

entrapped water in mixed RMs of different morphology has not been explored yet. We have also examined the change in the structural rigidity of water in RM of different shapes by Fourier transform infrared FTIR spectroscopy.

In order to investigate the mobility of the entrapped water molecules in the mixed RMs we have used a charge transfer probe, ANS (1-anilino-8-naphthalenesulfonic acid, ammonium salt), which resides close to the interface of the RM. However, it should be noted that the probe ANS is expected to have less affinity toward AOT head groups compared to that of the lecithin as both ANS and AOT are anionic in nature. The dynamics of solvation of the probe in the water-pool reveal the presence of various kinds of water molecules with different degrees of dynamical constraints. Selective excitation of another probe coumarin 500 (C-500) has also been used to investigate the mobility of water at the surfactant/isooctane/water interface. The exploration of the structural and dynamical properties of water molecules in the mixed reverse micellar system has importance in the better understanding of activity of enzymes [19] and synthesis of nanoparticles [20] in the mixed RMs, which is scarce in the present literature.

2. Material and methods

Chemicals are obtained from the following sources: sodium bis(2-ethylhexyl) sulfosuccinate (AOT, Sigma, Scheme 1), L-α-phosphatidylcholine (lecithin, Sigma, Scheme 1), 2,2,4-trimethyl pentane (isooctane, Sigma), coumarin 500 (C-500, Exciton, Scheme 1) and ANS (1-anilino-8-naphthalenesulfonic acid, ammonium salt, Sigma, Scheme 1). The chemicals are of highest commercially available purity and are used as received. All aqueous solutions are prepared using deionized water from Millipore system. AOT and lecithin are dissolved in isooctane to produce a 100 mM total surfactant concentration in isooctane,

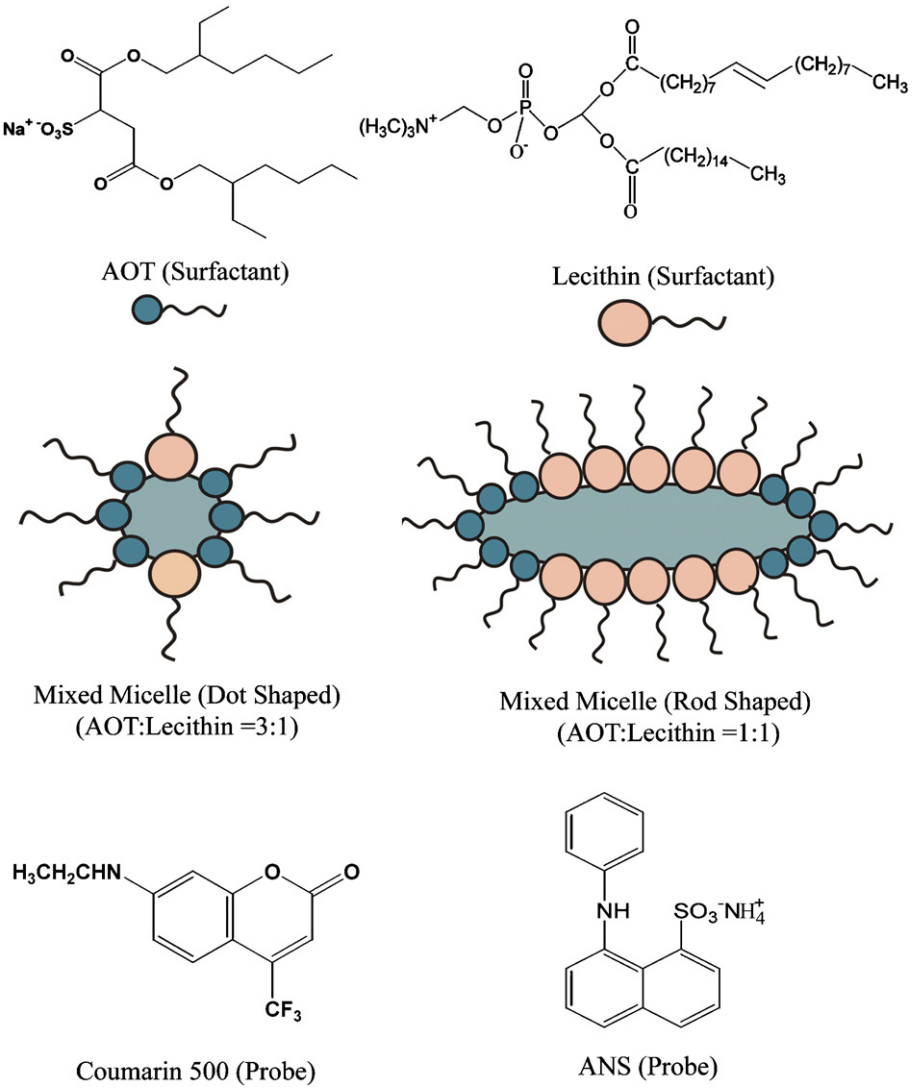

Scheme 1. Molecular structure of the anionic surfactant AOT and zwitterionic surfactant phospholipid L-α-phosphatidylcoline (lecithin), schematic picture of spherical reverse micelle, RM1 ([AOT]:[lecithin] = 3:1) and ellipsoidal reverse micelle, RM2 ([AOT]:[lecithin] = 1:1) & molecular structure of the probe coumarin 500 (C-500) and ANS.

and then same amount of water is injected into it to obtain RMs of different shapes with similar degree of hydration, w_0 ($w_0 = [\text{water}]/[\text{surfactant}] = 10$). Small angle neutron scattering (SANS) study [16] reveals that different packing parameters, P ($P = v/al$, where v is the volume occupied by the surfactant tails, a is the effective area of the head group and l is the maximum effective tail length) of AOT and lecithin drive a morphological change from spherical to ellipsoidal of the mixed RMs formed by these two surfactants. Lecithin forms interfacial film of lower curvature [21] due to its lower P value of 0.6 [16] than that of AOT ($P = 1.1$) [22], leading to prolate ellipsoidal droplets (Scheme 1) for a 1:1 molar ratio of AOT to lecithin. The shape changes to spherical when the [AOT]:[lecithin] = 3:1 with an aspect ratio close to unity as confirmed by the synthesis of spherical CdS nanoparticles in such mixed surfactant systems [23]. This is also supported by the experimental SANS data [16], which fits well by a model containing polydispersed spheres and reveals microemulsion droplets with an aspect ratio close to unity (i.e. spherical). Hence, the molar ratios of AOT to lecithin are maintained at 3:1 and 1:1 to obtain spherical (RM1) and ellipsoidal (RM2) RMs, respectively, as shown in Scheme 1.

Steady-state emission is measured with Jobin Yvon Fluoromax-3 fluorimeter. FTIR spectra are recorded on a JASCO FT/IR-6300 spectrometer (absorption mode) using CaF_2 window. DLS measurements are done with a Nano S Malvern instrument employing a 4 mW He–Ne laser ($\lambda = 632.8$ nm) equipped with a thermostatted sample chamber in which all the scattered photons from the sample are collected at 173° scattering angle. The scattering intensity data are processed using the instrumental software to obtain the hydrodynamic diameter (d_H) and the size distribution of the scatterer in each sample. Fluorescence transients have been measured and fitted by using commercially available spectrophotometer (LifeSpec-ps) from Edinburgh Instruments, UK (excitation wavelength 409 nm, 80 ps instrument response function (IRF)) with an attachment for temperature dependent studies (Julabo, Model-F32). To construct time-resolved emission spectra (TRES), we follow the technique described in Ref. [24]. The time dependent fluorescence Stokes shifts, as estimated from TRES are used to construct the normalized spectral shift correlation function or the solvent correlation function $C(t)$ defined as,

$$C(t) = \frac{v(t) - v(\infty)}{v(0) - v(\infty)}$$

where $v(0)$, $v(t)$ and $v(\infty)$ are the emission maxima (in cm^{-1}) at time zero, t and infinity, respectively. The $v(\infty)$ values have been taken to be the emission frequency beyond which insignificant or no spectral shift is observed. The $C(t)$ function represents the temporal response of the solvent relaxation process, as occurs around the probe following its photo excitation and the associated change in the dipole moment.

3. Results and discussion

Fig. 1 shows dynamic light scattering data of AOT/lecithin mixed RM, with different molar ratios of AOT to lecithin in isooctane. For [AOT]:[lecithin] = 3:1, the diameter and peak width are 10.3 and 4.45 nm, respectively. When [AOT]:[lecithin] is 1:1, the hydrodynamic diameter changes to 25.7 nm and width of the peak increases to 11.5 nm. These results are consistent with the previous DLS studies of mixed rod-like lecithin reverse micelles formed by dihexanophosphatidylcholine and diheptanoyl phosphatidylcholine [25]. The increase in the peak width with increase in lecithin concentration reflects the asymmetry in shape of the particle. Transmission electron microscopic (TEM) images of CdS nanoparticles synthesized in 1:1 [AOT]:[lecithin] mixed micelle reveal highly acicular quantum rod structure [20] of average width 4.1 ± 0.6 nm and length ranging from 50 to 150 nm. For nonspherical particle, the destructive interference of waves scattered from different points in the particle affects the autocorrelation function [26] of DLS data. Consequently, the hydrodynamic radius (R_h) of a sphere becomes equal to its actual radius, where the R_h of a rod is defined by the following equation [27,28], $R_h = \frac{L}{2s-0.19-8.24/s+12/s^2}$, here $s = \ln(L/r)$; L = length and r = radius of the rod. The R_h value of the RM2 obtained from our DLS study (12.9 nm) is in good agreement with the calculated value of R_h (12.8 nm) obtained on putting the L (70 nm) and r (4.5 nm, width of the particle obtained from TEM data + surfactant chain length) values from TEM data.

In order to explore the alteration of the structure of water with the change of reverse micellar morphology, we have performed FTIR spectroscopic studies. Using FTIR technique, it has been reported that water coexists in three [18,29] 'states' or 'layers' in the AOT RMs. Fig. 2a and b shows FTIR spectra of waters in the RMs with different morphology, particularly the intramolecular O–H stretching vibrations of water at ~3500 cm^{-1}. FTIR spectra of the solutions of different [AOT]:[lecithin] ratios (3:1 and 1:1) have been subtracted from the respective RMs in order to avoid the complexity in the interpretation of O–H

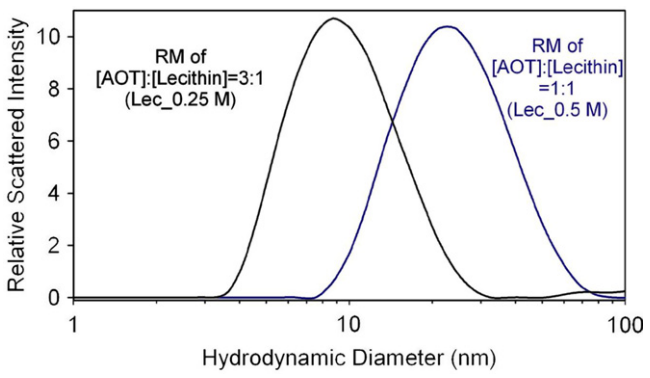

Fig. 1. Dynamic light scattering study shows hydrodynamic diameter of RM1 and RM2.

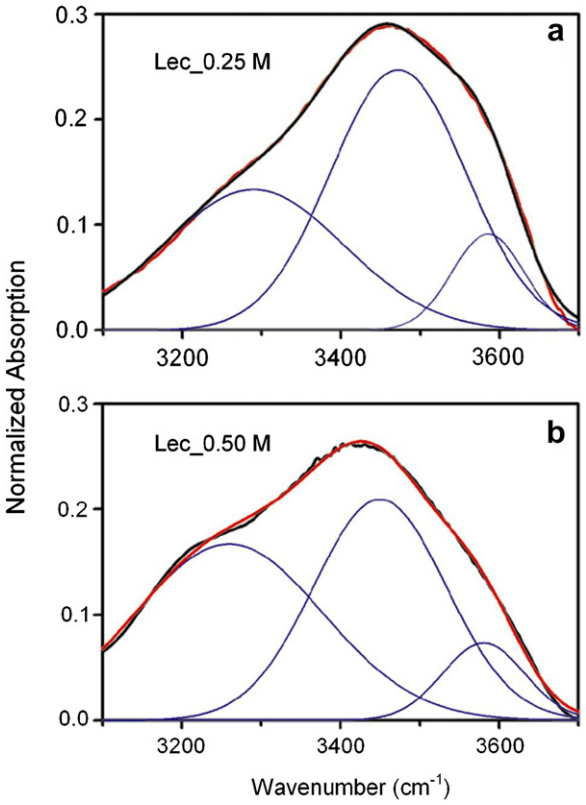

Fig. 2. FTIR spectra of: (a) spherical (Lec_0.25 M) and (b) ellipsoidal (Lec_0.50 M) RMs are shown. In order to identify various water structures in the RMs, spectral deconvolution according to three components Gaussian model has been performed.

stretching from that of the C–H bands. Multipeak deconvolution of relatively broad IR peak reveals the presence of different types of water in the RMs. The peaks obtained for water O–H have been fitted as a sum of Gaussian with the help of Gaussian curve fitting program, and the vibrational characteristics, particularly the peak area corresponding to each peak, has been analyzed using three-state models to *unravel* the nature of water inside the nanopool and the change in water properties with the change in the shape of RM. The broad bands obtained from FTIR studies (3100–3700 cm^{-1}) for different [AOT]:[lecithin] (3:1 and 1:1) have been fitted with three Gaussian peaks, which is in accordance with the three-state model [18,29,30]. The peaks at 3324 ± 20, 3479 ± 10 and $3587 \pm 20\ cm^{-1}$ (Fig. 2a and b) have been assigned to OH stretch in hydrogen-bonded-associated chains of water molecules in bulk water, hydrogen bonded dimers bound between the interface and bulk type water, and monomeric water or matrix isolated dimer in the close vicinity of interface, respectively. The comparison of the FTIR results between RM1 and RM2 demonstrates that the area fraction of bound type water increases (from 40% to 51%) and that of the free-type water decreases (from 50% to 42%) with the increase of lecithin concentration (which ultimately leads to morphological change from spherical to ellipsoidal) while the fraction of trapped water remains almost the same.

In order to investigate the dynamical properties of water inside the nanopool of RMs, we have followed picosecond-resolved solvation dynamics of a fluorescent probe ANS in the RMs. The fluorescence of the probe ANS is commonly used to monitor structural changes of proteins and membranes [31]. Fig. 3a shows fluorescence decay transients of ANS in spherical AOT/Lec RM at two different wavelengths. For both the RMs (RM1 and RM2) the fluorescence transients are found to decay at blue wavelengths and a corresponding rise is seen at red wavelengths. For

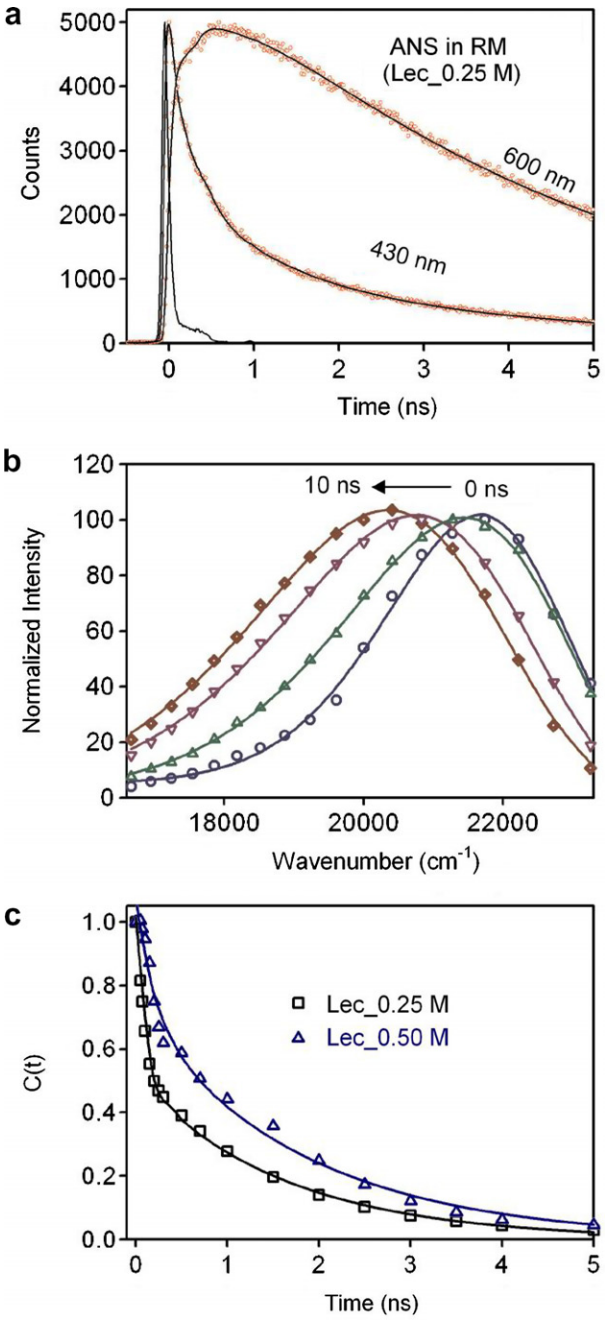

Fig. 3. (a) Fluorescence decay transients of ANS in RM1 (Lec_0.25 M). (b) Time-resolved emission spectra (TRES) of ANS in RM1. (c) Solvation correlation function, $C(t)$ of ANS in RM1 and RM2 (Lec_0.50 M).

RM1, ANS shows decay time constants of 0.06 ns (70%), 0.75 ns (21%) and 3.87 ns (9%) at 430 nm whereas, a rise component of 0.72 ns along with a decay component of 4.17 ns are observed at 600 nm. This observation is consistent with the clear case of solvation of ANS within the RM [32]. Time-resolved emission spectra (TRES) of ANS in RM1 are shown in Fig. 3b. The constructed solvent correlation functions (Fig. 3c) (with solvation shifts of 1190 cm^{-1} (RM1) and 1110 cm^{-1} (RM2)) show biexponential decay. For RM1 the $C(t)$ decays biexponentially with two time constants of 110 ps (49%) and 1.61 ns (51%). In the case of RM2, the decay of $C(t)$ also shows biexponential nature with time constants of 200 ps (31%) and 1.83 ns (72%). The faster and slower time constants of $C(t)$ for both the cases correspond to two types of water molecules present inside the pool of RM. These results are consistent with the study by Zhang and Bright [32], that reveals the different relaxation dynamics of interfacial and core associated water using the fluorescent probe ANS in AOT RM at low water content. The nanosecond solvation component of RM has been explained by Bhattacharyya and Bagchi [33] as the motion (both translation and rotation) of buried water, accompanied by cooperative relaxation of several surfactant chains. Such nanosecond solvation time has also been reported from our group recently using acridine orange in AOT RMs [34]. The lengthening of the fast solvent relaxation time constant (97–200 ps) is possibly due to the enhanced interaction of the relatively free-type water molecules with the interface of RM2 than that in the RM1 as evidenced from FTIR studies.

Selective excitation (409 nm) of another probe C-500 [35] has been employed to unravel the trapped interfacial water dynamics of RM. As demonstrated in an earlier study [35], the excitation wavelength of 409 nm only excites the population of C-500 in the close vicinity of polar environments of RMs. Fig. 4a shows that the decay pattern of C-500 in RM is strongly dependent on emission wavelength. The blue end decays with triexponential time constants of 0.10 ns (59.10%), 0.68 ns (31.80%) and 2.21 ns (9.10%) for RM1. A distinct rise component of 0.90 ns appears at the red wavelength (600 nm). The constructed TRES for RM1 and $C(t)$ for both RM1 and RM2 are shown in Fig. 4b and c, respectively. The $C(t)$ decays biexponentially with two time constants of 240 ps (54%) and 1.84 ns (46%). Fig. 4c reveals that the solvent response time scales for both the RMs are similar. The slower dynamical response (1.84 ns) is similar to that of the interfacial water molecules. These results depict that the probe molecule resides at the interface and the fraction of trapped water molecules remains nearly same for both the RMs. The observation is also supported from our FTIR data (Fig. 2).

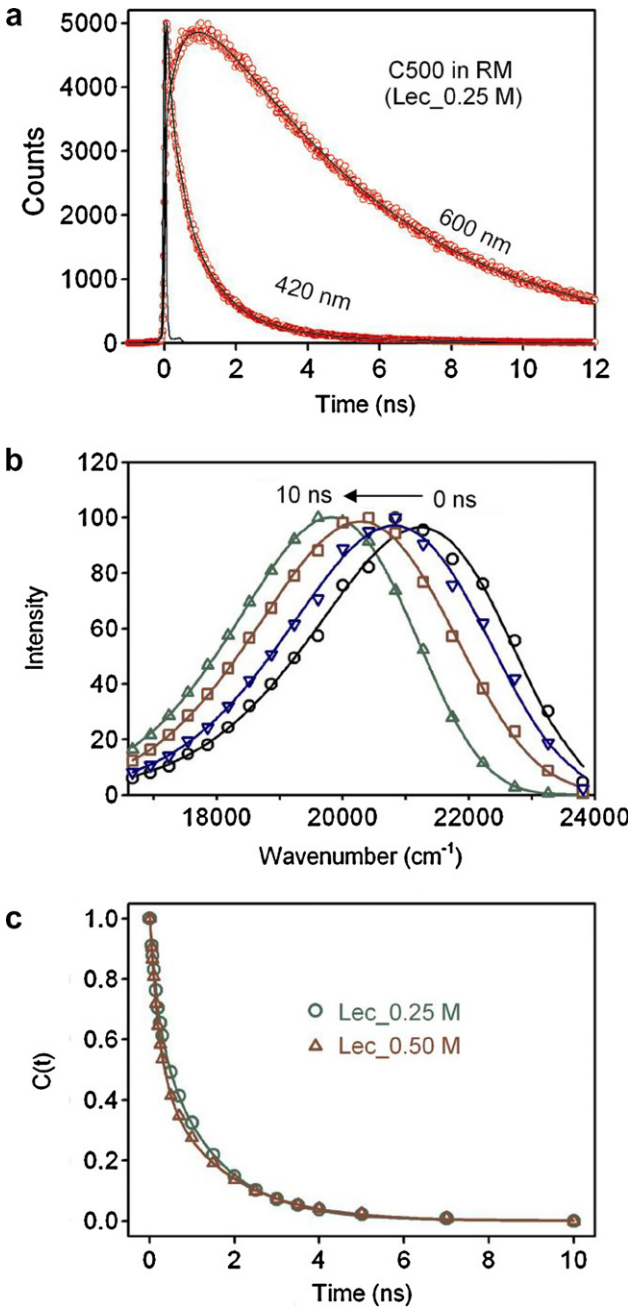

Fig. 4. (a) Fluorescence decay transients of C-500 in RM1 (Lec_0.25 M). (b) Time-resolved emission spectra (TRES) of C-500 in RM1. (c) Solvation correlation function, $C(t)$ of C500 in RM1 and RM2 (Lec_0.50 M).

4. Conclusion

We have studied the solvation dynamics of water molecules confined in the nanodroplets of mixed (AOT and lecithin) RMs of different morphology. DLS experiments confirm the alteration of morphology with the change in the relative molar ratio of AOT and lecithin in the RMs. FTIR studies together with picosecond-resolved fluorescence studies reveal that orientational and translational mobilities of water molecules vary from the interface to the core of RM due to different intermolecular interactions and different geometrical arrangements of the RMs. The mobility of trapped matrix isolated monomeric water molecules has also been investigated. The present study is important for understanding the structure and dynamics of water near a water–lipid interface.

Acknowledgements

S.S.N. and R.S. thank CSIR and UGC, India, respectively, for fellowships. We thank Dr. Rajib K. Mitra for fruitful discussions. We express our gratitude to DST for financial grant (SR/FTP/PS-05/2004).

References

[1] A.M. Dokter, S. Woutersen, H.J. Bakker, Proc. Natl. Acad. Sci. USA 103 (2006) 15355.
[2] N.E. Levinger, Science 298 (2002) 1722.
[3] D.M. Willard, R.E. Riter, N.E. Levinger, J. Am. Chem. Soc. 120 (1998) 4151.
[4] P. Sen, S. Mukherjee, A. Halder, K. Bhattacharyya, Chem. Phys. Lett. 385 (2004) 357.
[5] K. Bhattacharyya, Acc. Chem. Res. 36 (2003) 95.
[6] I.R. Piletic, D.E. Moilanen, N.E. Levinger, M.D. Fayer, J. Am. Chem. Soc. 128 (2006) 10366.
[7] R.E. Riter, D.M. Willard, N.E. Levinger, J. Phys. Chem. B 102 (1998) 2705.
[8] N. Sarkar, K. Das, A. Datta, S. Das, K. Bhattacharyya, J. Phys. Chem. 100 (1996) 10523.
[9] G.B. Dutt, J. Phys. Chem. B 106 (2002) 7398.
[10] J. Faeder, B.M. Ladanyi, J. Phys. Chem. B 194 (2000) 1033.
[11] F. Sterpone, G. Marchetti, C. Pierleoni, M. Marchi, J. Phys. Chem. B 110 (2006) 11504.
[12] S. Abel, M. Waks, W. Urbach, M. Marchi, J. Am. Chem. Soc. 128 (2006) 382.
[13] D. Pant, R.E. Riter, N.E. Levinger, J. Chem. Phys. 109 (1998) 9995.
[14] D.M. Willard, N.E. Levinger, J. Phys. Chem. B 104 (2000) 11075.
[15] M. Bergstrom, J.S. Pedersen, Langmuir 14 (1998) 3754.
[16] B. Simmons, V. Agarwal, G. McPherson, V. John, A. Bose, Langmuir 18 (2002) 8345.
[17] L.P. Novaki, O.A. El Seoud, J. Colloid Interf. Sci. 202 (1998) 391.
[18] T.K. Jain, M. Varshney, A. Maitra, J. Phys. Chem. 93 (1989) 7409.
[19] C.-L. Chiang, Biotechnol. Techn. 13 (1999) 453.
[20] B.A. Simmons, S. Li, V.T. John, G.L. McPherson, A. Bose, W. Zhou, J. He, Nano Lett. 2 (2002) 263.
[21] S.Y. Shiao et al., Colloids Surf. A 128 (1996) 197.
[22] T.K. De, A. Maitra, Adv. Colloid Interf. Sci. 59 (1995) 95.
[23] M.-I. Baraton, Synthesis Functionalization and Surface Treatment of Nanoparticles, American Scientific Publishers, California, 2003.
[24] M.L. Horng, J.A. Gardecki, A. Papazyan, M. Maroncelli, J. Phys. Chem. 99 (1995) 17311.
[25] T.-L. Lin, Y. Hu, W.-J. Liu, Langmuir 13 (1997) 1422.
[26] A.G. MacDiarmid, S.K. Tripathy, J. Kumar, H.S. Nalwa, Handbook of Polyelectrolytes and their Applications, Americal Scientific Publishers, USA, 2000.
[27] E. Kokufuta, K. Ogawa, R. Doi, R. Kikuchi, R.S. Farinato, J. Phys. Chem. B 111 (2007) 8634.
[28] S. Broersma, J. Chem. Phys. 32 (1960) 1626.
[29] A. Maitra, T.K. Jain, Z. Shervani, Colloids Surf. 47 (1990) 255.
[30] G. Onori, A. Santucci, J. Phys. Chem. 97 (1993) 5430.
[31] S.K. Pal, J. Peon, A.H. Zewail, Proc. Natl. Acad. Sci. USA 99 (2002) 15297.
[32] J. Zhang, F.V. Bright, J. Phys. Chem. 95 (1991) 7900.
[33] K. Bhattacharyya, B. Bagchi, J. Chem. Sci. 119 (2007) 113.
[34] A.K. Shaw, S.K. Pal, J. Phys. Chem. B 111 (2007) 4189.
[35] P. Majumder, R. Sarkar, A.K. Shaw, A. Chakraborty, S.K. Pal, J. Colloid Interf. Sci. 290 (2005) 462.